

QSAR and Molecular Docking Studies of Pyrazolyl-thiazolinone Derivatives as Antitumor Activity. Computational studies of pyrazolyl-thiazolinone derivatives.

¹Shruti Suryawanshi, ²Dr. Trupti Chitre, ³Dr. Santosh Gandhi, ⁴Mrs. Kalyani Asgaonkar.

¹Research Student, ^{2,3}Associate Professor, ⁴Assistant professor

¹Department of Pharmaceutical Chemistry,

¹All India Shri Shivaji Memorial Society's College of Pharmacy, Kennedy Road, Near R.T.O., Pune-411001, M.S., India.

Abstract :

Background: Cancer is a leading cause of death worldwide. Pyrazoles, thiazoles and fused thiazoles have been reported to possess many biological activities including anticancer activity.

Aims and Objectives: To study 2D and 3D QSAR followed by Molecular Docking studies to generate new chemical entities (NCE's) containing pyrazolyl-thiazolinone as pharmacophore for anticancer activity.

Materials and methods: In the presented studies we have reported the results of QSAR studies for the 36 derivatives of pyrazolyl-thiazolinone synthesized by Ke-Ming Qiu et.al. 2D and 3D QSAR studies were done by using V Life software. The NCE's were designed by using Lead grow tool in V Life Software and screened by Lipinski screen. The designed compounds having the Lipinski score 5 were subjected to molecular docking studies with EGFR Kinase enzyme by using Schrodinger software.

Result and Discussion: The r^2 and q^2 for the 2D QSAR and 3D QSAR was found to be 0.781 and 0.709 respectively. By performing docking studies, we established that most of the molecules showed the good binding energy and the docking score. Molecule 1 and 3 have the highest dock score with good binding energy.

Conclusion: The molecule 1 and 3 are the significant molecules developed from the results of QSAR and molecular docking studies and they have potential to act as anticancer agent.

Keywords - pyrazolyl-thiazolinone, Antitumor, 2D-3D QSAR, Docking.

I. INTRODUCTION –

Cancer is a leading cause of death worldwide, accounting for nearly 10 million deaths in 2020. (WHO report 2020) [1]. Various pyrazole derivatives have been reported to have a broad spectrum of biological activities such as antiviral/antitumor [2,3], antibacterial [4,5], anti-inflammatory [6], analgesic [7], fungistatic [8], and anti-hyperglycaemic activity [9]. Similarly, Thiazolinone have also exhibited a wide spectrum of biological activities such as anti-inflammatory, antimicrobial, antiproliferative, antiviral, anticonvulsant, antifungal, and antibacterial [10,11,12].

Both these scaffold together as a hybrid have been reported to possess EGFR and HER-2 kinase inhibitory activity [13]. QSAR is a powerful tool for drug design. It gives the idea about the relationship of chemical structure and biological activity [14,15]. In present study we have attempted to optimize the Pyrazole- Thiazolinone pharmacophore for anticancer activity by two dimensional (2D) and three-dimensional Quantitative structure activity relationship (3D QSAR). New compounds were designed by using Combilib tool in V-Life software and were screened by Lipinski filter. The compounds having the Lipinski score of 5 were subjected to the molecular docking process by using the Schrodinger software.

II. MATERIAL AND METHODS –

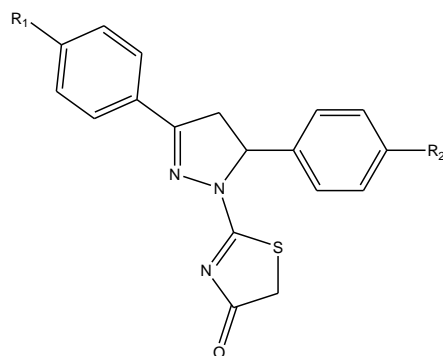
2.1 MATERIALS -

All the molecular modelling studies (2D, 3D QSAR and Lead grow) were carried out by using the software V life MDS (V Life MDS 4.4). The molecular docking studies were carried out by using the Schrodinger Software. [16,17,15] The structure of all the compounds were sketched by using Chem Draw Ultra 8.0 software. The 3D optimization and energy minimization step were performed by using the Chem Draw 3D Ultra 8.0 software.

DATA SET –

Data set of 36 derivatives of pyrazolyl-thiazolinone with antitumor activity reported by Ke-Ming Qiu et.al was used for QSAR studies. Biological activity is expressed in terms of minimum inhibitory concentration (MIC) was converted into pMIC [pMIC = -log(MIC)] [13]

For development of QSAR model, entire data set was divided into training set (to generate the regression models) and test set (to evaluate the predictive ability of these models). The test compounds were selected manually based on structural diversity and distribution of their antitumor activity. Uni-Column statistics for training set and test set were generated to check correctness of selection criteria for training and test set molecules. The antitumor activities expressed as pMIC values were used as dependent variables in the QSAR analyses while the molecular descriptors served as the independent variables. [16,17].

Table 1 – Data set for 36 molecules for QSAR study.^[13]

Compound Number	R ₁	R ₂	IC ₅₀ (μM)	pIC ₅₀ (μM)
E1	-H	-H	3.38	5.4710
E2 ¹	-H	-F	4.86	5.3133
E3	-H	-Cl	3.49	5.4571
E4	-H	-Br	1.35	5.8696
E5	-H	-Me	3.03	5.5185
E6	-H	-OMe	4.27	5.3695
E7 ¹	-F	-H	8.14	5.0893
E8	-F	-F	16.92	4.7715
E9	-F	-Cl	10.92	4.9617
E10	-F	-Br	4.79	5.3196
E11	-F	-Me	8.36	5.0777
E12 ^{1,2}	-F	-OMe	10.69	4.9710
E13 ²	-Cl	-H	5.34	5.2724
E14 ²	-Cl	-F	14.21	4.8474
E15 ^{1,2}	-Cl	-Cl	8.16	5.0883
E16 ²	-Cl	-Br	2.28	5.6420
E17 ^{1,2}	-Cl	-Me	6.67	5.1758
E18 ²	-Cl	-OMe	8.58	5.0665
E19 ²	-Br	-H	3.20	5.4948
E20 ¹	-Br	-F	6.48	5.1884
E21	-Br	-Cl	4.12	5.3851
E22	-Br	-Br	2.03	5.6925
E23	-Br	-Me	5.58	5.2533
E24 ^{1,2}	-Br	-OMe	7.96	5.0990
E25	-Me	-H	1.08	5.9665
E26	-Me	-F	2.01	5.6968
E27	-Me	-Cl	1.66	5.7798
E28	-Me	-Br	0.24	6.6197
E29	-Me	-Me	1.16	5.9355
E30	-Me	-OMe	4.24	5.3726
E31	-OMe	-H	2.37	5.6252
E32	-OMe	-F	5.95	5.2254
E33	-OMe	-Cl	5.35	5.2716
E34	-OMe	-Br	1.26	5.8996
E35 ¹	-OMe	-Me	5.46	5.2628
E36	-OMe	-OMe	8.89	5.0510

(1 - test set of 2D QSAR, 2 - test set of 3D QSAR).

2.2 Methods -

2.2.1 2D QSAR –

For generation of 2D QSAR models, methods such as partial least square (PLS), multiple linear regression (MLR) and principal component regression (PCR) were used. Various descriptors such as physicochemical and alignment were utilized to develop the structure-activity relationship. The biological activity is used as dependent variable and the generated descriptors are used as

independent variable. Statistical parameters such as correlation coefficient (r^2), Cross-validated correlation coefficient (q^2), predicted r^2 , r^2_{se} , Alpha Rand Predicted r^2 , etc. were used to evaluate the QSAR model. [17]

2.2.2 3D QSAR –

The 3D QSAR models were generated by k nearest neighbour molecular field analysis (kNN MFA) using simulated annealing (SA) variable selection method. The optimized molecules were aligned by using a template-based alignment method (fig 1). The resulting set of molecules was used for generation of 3D QSAR model. This was followed by generation of rectangular grid around the molecule. The steric, hydrophobic and electrostatic interaction energies were computed at the lattice point of the grid. Further the generated QSAR model was evaluated by using various statistical parameters. [18].

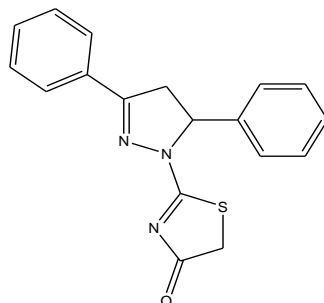


Fig 1 – Common template used for alignment of pyrazolyl-thiazolinone derivatives.

2.2.3 DESIGN OF NEW CHEMICAL ENTITIES (NCE'S) USING LEADGROW TOOL –

Information and correlation of structure with activity obtained from QSAR studies guided us to design the NCE's by using combilib tool in V Life MDS software. Large library of the compounds having the pyrazolyl-thiazolinone nucleus were designed and screened through the Lipinski rule. Based on their Lipinski score the designed NCE's were selected for further docking study.[14]

2.2.4 MOLECULAR DOCKING -

The designed NCE's with a Lipinski score 5 were subjected to molecular docking studies using Schrodinger software. To know the binding affinity and mode of interaction, the ligands were docked into the active site of EGFR kinase (PDB Code 1M17), which was downloaded from the Protein Data Bank (www.rcsb.org).

The protein was prepared by removing all the water molecules and addition of hydrogen atoms. The prepared ligand and protein were used for further docking process. The ligand is flexible and the receptor are rigid but the protein active site is slightly flexible. The dock score was generated and the molecules having highest dock score was selected. [17,18]. The binding energy and the Binding pattern of all the molecules was studied.

III. RESULT AND DISCUSSION -

3.1 2D QSAR -

The results for 2D QSAR were obtained by various methods amongst them the MLR (Multiple regression method) has shown the best results. The following equation was generated from the results and it was considered for new chemical entities generation. $PIC50 = 0.5909 (T_2_C_6) + 0.0928 (SaaCHE-index) - 0.0304 (PolarSurfaceAreaExcludingPandS) + 0.3769 (SsBrE-index) \dots \dots \dots Eq. 1$

The generated model was cross validated. These parameters were more significant than those generated by the other methods. (Table 2). Graph of contributed descriptors is depicted in figure 1. Also, the plot of actual versus predicted activity of training set and test set is shown in figure 2. The comparative graph for predicted and actual activity of test set and training set is shown in figure 3 and 4 respectively.

Table 2 – Results of generated 2D QSAR model by MLR method.

Statistics parameter	Score
Optimum Components	3
n	29
Degree of freedom	25
r^2	0.7814
q^2	0.6699
F test	29.7801
r^2_{se}	0.1932
q^2_{se}	0.2374
Pred_ r^2	0.8813

Pred_ r ² _se	0.1148
ZScore r ²	7.00534
ZScore q ²	7.83529
Best Rand r ²	0.30327
Best Rand q ²	-0.09130
Alpha Rand r ²	0.00000
Alpha Rand q ²	0.00000
Z Score Pred r ²	2.14665
Best Rand Pred r ²	0.39951
Alpha Rand Pred r ²	0.05000
Descriptors	T_2_C_6 SaaCHE-index PolarSurfaceAreaExcludingPandS SsBrE-index
Coefficients	0.5909 0.0928 -0.0304 0.3769

Fig. 1 - Contribution of descriptors.

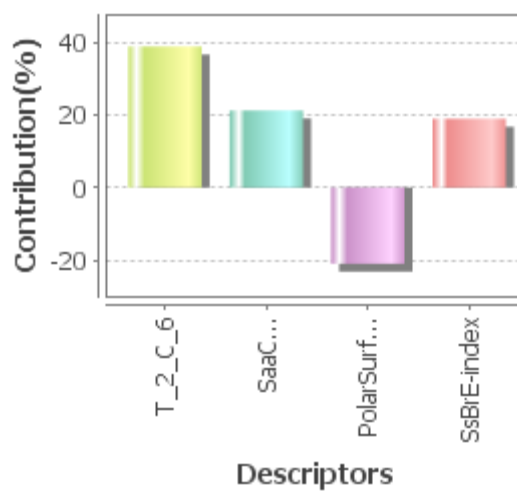


FIG. 2 - PLOT OF ACTUAL VERSUS PREDICTED ACTIVITY OF TRAINING SET AND TEST SET OF SA-MLR METHOD

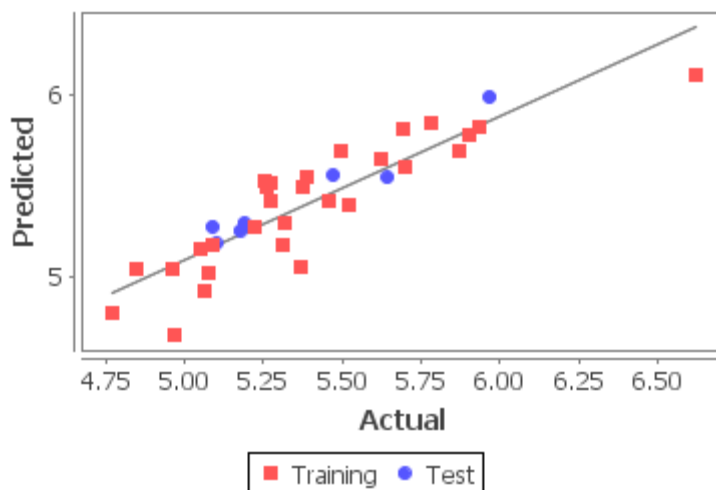


Fig 3 – Actual and predicted activity of test set.

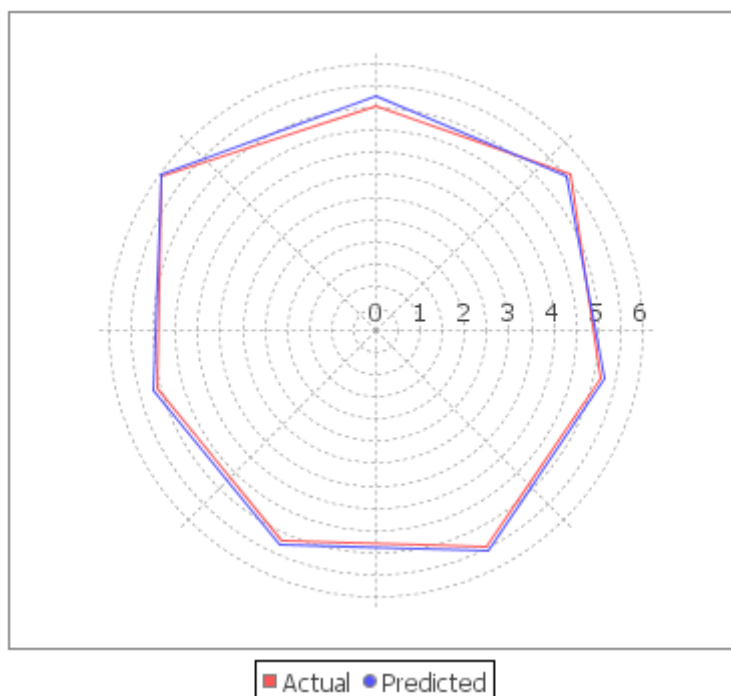
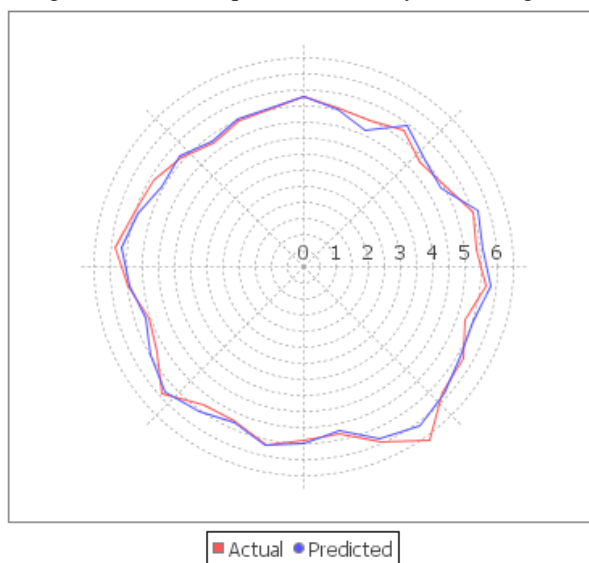


Fig 4 – Actual and predicted activity of training set.



An idea about the requirement of different physicochemical descriptors and alignment descriptors and their contribution for antitumor activity was obtained from the 2D QSAR analysis. T_2_C_6 (i.e., the count of number of double bounded atoms separated from oxygen atom by 7 bonds in a molecule), SaaCHE-index (Electrotopological state indices for number of -CH group connected with two aromatic bonds) and SsBrE-index (Electrotopological state indices for number of bromines connected with one single bond) contributes positively towards the activity in the formation of the new chemical entities. PolarSurfaceAreaExcludingP and S (the descriptors signify total polar surface area excluding P and S) contributes negatively in the activity.

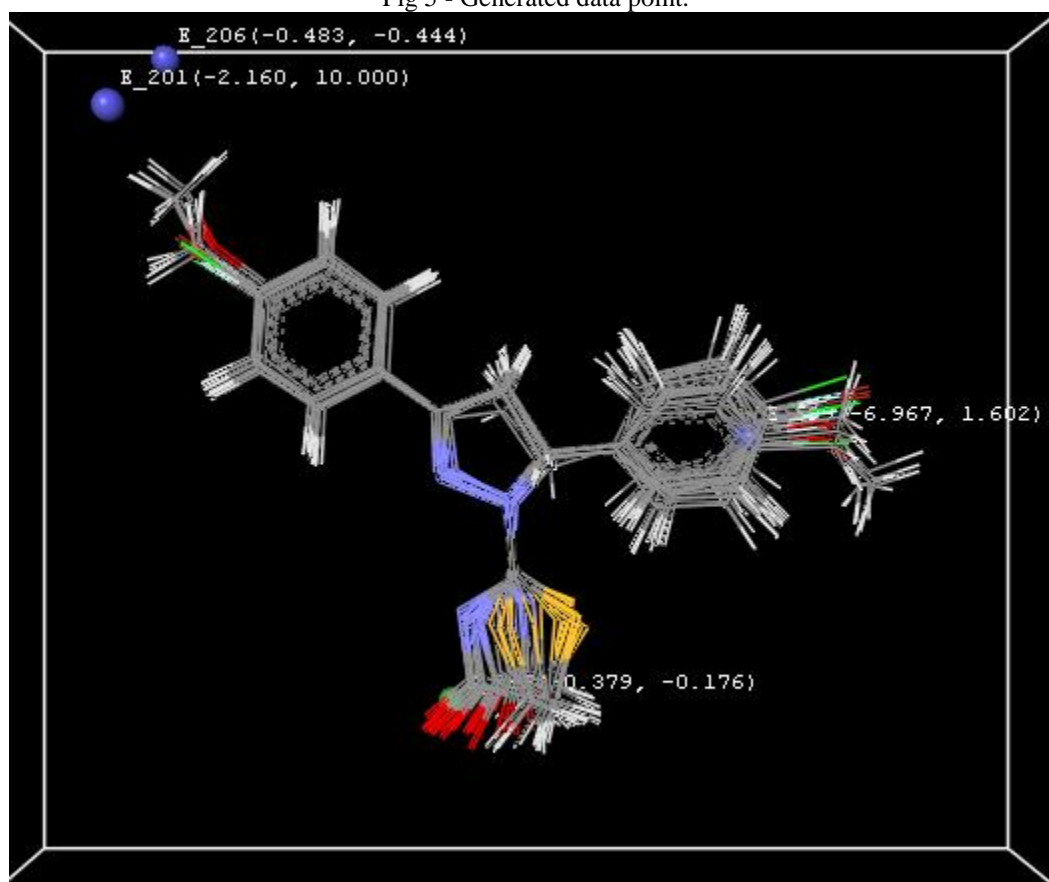
3.2 3D QSAR –

In continuation with the 2D QSAR, 3D QSAR models were also generated to predict and interpret the activity. The 3D QSAR was performed by using 8 molecules as test set and remaining 28 molecules as training set. The KNN method was used for performing the 3D QSAR. Various parameters such as q^2 , q^2_{se} etc. were used for selection of best models using 2 fields i.e., steric and electrostatic. The results of 3D QSAR are included in table 3 and the generated data points are shown in figure 5.

Table 3 – Results of 3D QSAR.

Statistical Parameters	SA-KNN Score
k Nearest Neighbour	2
n	28
Degree of Freedom	23
q^2	0.7093
q^2_{se}	0.2096
Pred_r ²	0.3237
Pred_r ² se	0.2871

Fig 5 - Generated data point.



3.3 DESIGN OF NCE'S CONTAINING PYRAZOLYL-THIAZOLINONE PHARMACOPHORE –

More than 500 compounds were generated using combilib tool of V-Life software which follows the Lipinski rule. Only 13 most active molecules (Table 4) on the basis of their Lipinski score was selected for the further process. The various descriptors were generated in Lead grow tool result i.e. H-Acceptor Count which indicates Number of hydrogen bond acceptor atoms, molecular weight signifies the molecular weight of the compound.

Table 4 - Structure of NCE's with Lipinski parameters

Molecule no.	39	40	41	42	43	44
1	f	allyl	k	Cyclobutane	Vinyl	Cyclohexane
2	f	s	k	Cyclobutane	Br	Cyclohexane
3	f	s	k	Cyclobutane	Br	-O-CH ₃
4	f	s	k	Cyclobutane	Vinyl	Cyclohexane
5	f	s	k	Cyclobutane	Vinyl	-O-CH ₃
6	f	s	k	Cyclohexane	Br	Cyclohexane
7	f	s	k	Cyclohexane	Br	Acetate
8	f	s	k	Cyclohexane	Vinyl	Cyclohexane
9	f	allyl	k	Cyclobutane	Br	Cyclohexane
10	f	allyl	k	Cyclobutane	Br	-O-CH ₃
11	f	allyl	k	Cyclohexane	Br	Cyclohexane
12	f	allyl	k	Cyclohexane	Br	-O-CH ₃
13	f	s	k	Cyclohexane	Br	Acetate

Molecule no.	H-Acceptor Count	Mol. Wt.	Polar Surface Area	Screen Score
1	1	607.87	70.86	5
2	3	652.73	109.66	5
3	4	600.61	118.89	5
4	3	599.87	109.66	5
5	4	547.75	118.89	5
6	3	680.79	109.66	5
7	4	628.67	118.89	5
8	3	627.93	109.66	5
9	2	660.73	70.86	5
10	3	608.61	80.09	5
11	2	688.78	70.86	5
12	3	636.66	80.09	5
13	5	656.68	135.96	5

3.4 MOLECULAR DOCKING STUDIES –

Molecular docking studies give the information about the interactions between the Ligand and the Protein molecule. Therefore, all designed NCE's were docked with active site of the enzyme EGFR kinase. Dock score of compounds 1 and 3 were found to be -5.18kcal/mol and -5.21kcal/mol respectively. These values are comparable with the value of binding energy of standard drug i.e., Erlotinib (-4.63 kcal/mol). The binding energy of all the new designed compounds was better than the standard. Molecule 2 and 4 was having the highest binding energy. This indicates that the new designed compound has a better binding affinity with the EGFR kinase enzyme. The dock score, No. of hydrogen bonds, distance in A⁰ and binding energy of all the 7 molecules is included in the table 5.

Molecule no.	No. of hydrogen bonds	Atom forming H bond	H bond interaction with	Distance in A ⁰	G Score (kcal/mol)	Binding Energy (kcal/mol)
1 (206)	2		Met769	2.80	-5.18	-48.59
2 (458)	2		Gly695	2.81	-4.84	-51.56
3 (459)	3		Gln767	2.80	-5.21	-48.07
4 (462)	1		Lys721	2.81	-5.01	-49.69
5 (463)	2		Met769	2.80	-4.87	-47.76
6 (474)	2		Met769	2.80	-5.15	-49.50
7 (475)	2		Ala719	2.80	-4.92	-47.97
8 (478)	3	O, H, H	Asp831, Met769, H ₂ O			
9 (202)					-4.62	-47.97
10 (203)						
11 (218)						
12 (219)						
13 (476)						
Erlotinib (standard)	2		Lys721	1.09	-4.63	-47.16

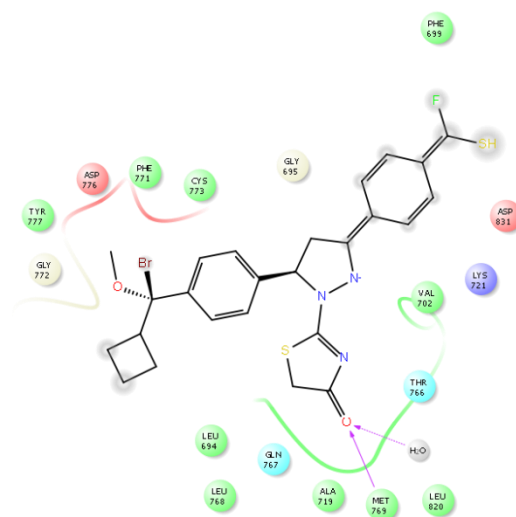


Fig 6 – Interaction of molecule 3 with EGFR Kinase

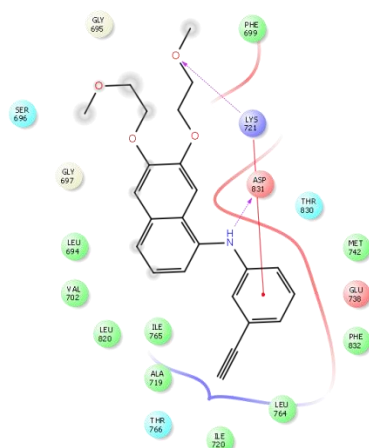


Fig 8 - Interaction of Erlotinib (standard) with EGFR Kinase

IV. CONCLUSION –

In the present study 36 derivatives of pyrazolyl-thiazolinone synthesized by Ke-Ming Qiu et.al were studied using 2D and 3D QSAR, for pharmacophore optimization for antitumor activity. Best model generated showed correlation coefficient $r^2 = 0.7814$ and $q^2 = 0.6699$ for 2D QSAR and $q^2 = 0.7093$ for 3D QSAR. Therefore, the new chemical entities were designed based on their various properties such as electrostatic, steric, hydrophobic and topological requirements. The substitution pattern is based upon the 2D and 3D QSAR studies. Thus, the library of pyrazolyl-thiazolinone derivatives was designed based on QSAR results and screened through the Lipinski screen. The molecules with higher Lipinski score subjected to molecular docking studies and the binding affinity of the molecules with EGFR Kinase was reported. Molecules 1 and 3 is having the highest binding affinity with EGFR kinase. Molecule 2 and 4 is having highest binding energy.

V. ACKNOWLEDGMENT

The authors are thankful to Dr. Ashwini R. Madgulkar, Principal, AISSMS College of Pharmacy, for continuous motivation, support and providing necessary infrastructure to carry out this work. We thank Schrodinger Software team for providing us the demo version of the Schrodinger Software.

REFERENCES

1. World Health Organization, 2020, Global Anticancer Report.
2. Manfredini, S.; Bazzanini, R.; Baraldi, P. G.; Guarneri, M.; Simoni, D.; Marongiu, M. E.; Pani, A.; Tramontano, E.; La Colla, P. Pyrazole-related nucleosides. Synthesis and antiviral/antitumor activity of some substituted pyrazole and pyrazolo[4,3-d]-1,2,3-triazin-4-one nucleosides. *J. Med. Chem.* **1992**, 35, 917.
3. Park, H.-A.; Lee, K.; Park, S.-J.; Ahn, B.; Lee, J.-C.; Cho, H. Y.; Lee, K.-I. antitumor activity of pyrazole oxime ethers. *Bioorg. Med. Chem. Lett.* **2005**, 15, 3307.
4. Tanitame, A.; Oyamada, Y.; Ofuji, K.; Fujimoto, M.; Iwai, N.; Hiyama, Y.; Suzuki, K.; Ito, H.; Wachi, M.; Yamagishi, J. Design, synthesis and structure-activity relationship studies of novel indazole analogues as DNA gyrase inhibitors with Gram-positive antibacterial activity. *J. Med. Chem.* **2004**, 47, 3693.

5. Kucukguzel, S. G.; Rollas, S.; Erdeniz, H.; Kiraz, M.; Ekinci, A. C.; Vidin, A. Synthesis, Characterization and pharmacological properties of some 4- arylhydrazono-2-pyrazoline-5-ones derivatives obtained from heterocyclic amine, *Eur. J. Med. Chem.* **2000**, 35, 761.
6. Penning, T. D.; Talley, J. J.; Bertenshaw, S. R.; Carter, J. S.; Collins, P. W.; Docter, S.; Graneto, M. J.; Lee, L. F.; Malecha, J. W.; Miyashiro, J. M.; Rogers, R. S.; Rogier, D. J.; Yu, S. S.; Anderson, G. D.; Burton, E. G.; Cogburn, J. N.; Gregory, S. A.; Koboldt, C. M.; Perkins, W. E.; Seibert, K.; Veenhuizen, A. W.; Zhang, Y. Y.; Isakson, P. C. Synthesis and biological evaluation of the 1,5-diarylpyrazole class of cyclooxygenase-2 inhibitors: Identification of 4-[5-(4-methylphenyl)-3(trifluoromethyl)-1h-pyrazol-1-yl]benzenesulfonamide (sc-58635, celecoxib), *J. Med. Chem.* **1997**, 40, 1347.
7. Patricia D.Sauzem, PabloMachado, Maribel A.Rubin, Gabrielada S. Sant'Anna, Henrique B.Faber, Alessandra H.de Souza, Carlos F.Mello, PauloBeck, Robert A.Burrow, Helio G.Bonacorso, NiloZanatta, Marcos A.P.Martin , Design and microwave-assisted synthesis of 5-trifluoromethyl-4,5-dihydro-1H-pyrazoles: Novel agents with analgesic and anti-inflammatory properties, *European journal of Medicinal Chemistry*, **2008**, 43(6),1237-1247.
8. Sridhar, R.; Perumal, P. T.; Etti, S.; Shanmugam, G.; Ponnuswamy, M. N.; Prabavathy, V. R.; Mathivanan, N. Design, synthesis and anti-microbial activity of 1H-pyrazole carboxylates, *Bioorg. Med. Chem. Lett.* **2004**, 14, 6035.
9. Bebernitz, G. R.; Argentieri, G.; Battle, B.; Brennan, C.; Balkan, B.; Burkey, B. F.; Eckhardt, M.; Gao, J.; Kapa, P.; Strohschein, R. J.; Schuster, H. F.; Wilson, M.; Xu, D. D. The effect of 1,3-diaryl-[1H]-pyrazole-4-acetamides on glucose utilization in ob/ob mice, *J. Med. Chem.* **2001**, 44, 2601.
10. Ottana, R.; Maccari, R.; Barreca, M. L.; Bruno, G.; Rotondo, A.; Rossi, A.; Chiricosta, G.; Di Paola, R.; Sautebin, L.; Cuzzocrea, S.; Vigorita, M. G. 5-Arylidene-2-imino-4-thiazolidinones: design and synthesis of novel anti- inflammatory agents, *Bioorg. Med. Chem.* **2005**, 13, 4243.
11. Gududuru, V.; Hurh, E.; Dalton, J. T.; Miller, D. D. Synthesis and antiproliferative activity of 2-aryl-4-oxo-thiazolidin-3-yl-amides for prostate cancer, *Bioorg. Med. Chem. Lett.* 2004, 14, 5289.
12. Rydzik, E.; Szadowska, A.; Kaminska, A. Synthesis of benzylidene derivatives of 3-o, 3-m and 3-p-chlorophenylhydantoin and the study of their anticonvulsant action, *Acta Pol. Pharm.* **1984**, 41, 459.
13. Ke-Ming Q; Hai-Hong W; Li-Ming W; Yin L; Xian-Hui Y; Xiao-Ming W; Hai-Liang Z. Design, synthesis and biological evaluation of pyrazolyl-thiazolinone derivatives as potential EGFR and HER-2 kinase inhibitors, *Bioorganic & Medicinal Chemistry*, **2012**, 20 2010-2018.
14. Chitre T; Patil S; Sujalegaonkar A; Asgaonkar K. Designing of Thiazolidin-4-one Pharmacophore using QSAR Studies for Anti-HIV Activity, *Indian Journal of Pharmaceutical Education and Research*, **2021**, 55(20), 581-589.
15. Chitre T; Asgaonkar K; Patil S; Kumar S; Khedkar V; Garud D. QSAR, docking studies of 1,3-thiazinan-3-yl isonicotinamide derivatives for antitubercular activity. *Computat Biol and Chem.* **2017**, 68, 211-218.
16. Vlife MDS SUITS manual version 4.4.
17. Patil S; Asgaonkar K; Chitre T; Bhat V; Ethape S; Sujalegaonkar A; Bhalekar S. 2D and 3D QSAR of Benzimidazole Analogues as Novel HIV-1 Non Nucleoside Reverse Transcriptase Inhibitors, *Indian Journal of Pharmaceutical Education and Research* ,**2017**, 51(2), 122-128.
18. Noolvi M; Patel H. A comparative QSAR analysis and molecular docking studies of quinazoline derivatives as tyrosine kinase (EGFR) inhibitors: A rational approach to anticancer drug design, *Journal of Saudi Chemical Society.* 2013, 17(4), 361-379.